

## Supplementary Material

### I. EXPERIMENTAL ASPECTS

Experimental results regarding the full Heusler compound  $\text{Fe}_2\text{VAl}$  have been obtained as described in detail in Ref. 1. A 5 g sample was prepared by high frequency melting, followed by a heat treatment of the specimen under vacua at  $900^\circ\text{C}$  for one week. From X-ray patterns the phase purity was checked. The lattice parameter at room temperature was obtained as  $a = 5.766\text{\AA}$  in good agreement to previous  $\text{Fe}_2\text{VAl}$  samples.

### II. DENSITY OF STATES OF PURE Fe AND $\text{Fe}_2\text{VAl}$

Inspecting crystal structure of  $\text{Fe}_2\text{VAl}$  in Fig.1, one realizes that –if all the atoms would be Fe– it is a fourfold supercell of bcc Fe. The measured cubic lattice parameter of  $5.766\text{\AA}$  for  $\text{Fe}_2\text{VAl}$  is rather close to  $2 \times 2.87 = 5.74\text{\AA}$ , which is twice the measured lattice parameter of bcc ferromagnetic Fe. However, in  $\text{Fe}_2\text{VAl}$  the Fe atoms carry no local magnetic moment. We estimate the influence of the Fe local magnetic moments on the lattice spacing by comparing VASP calculations for non-spin polarized bcc Fe ( $a = 2.74\text{\AA}$ ) to spin-polarized bcc Fe ( $a = 2.81\text{\AA}$ ), indicating a reduction of  $a$  by 2.5 % for the non-polarized case. The rather equal lattice parameters of non-magnetic  $\text{Fe}_2\text{VAl}$  and  $4 \times \text{bcc}$  magnetic Fe (for both, measurement and DFT calculations) originate from the larger atomic volume of Fe in the compound case ( $15.06\text{\AA}^3$  as compared to  $11.1\text{\AA}^3$  for magnetic bcc Fe) and the smaller volumes of V and Al (Table 1). The atomic volume of Al is rather small because of the significant reduction of valence electronic charge, whereas the rather large atomic volume of Fe in the compound is due to the significant gain in electronic charge.

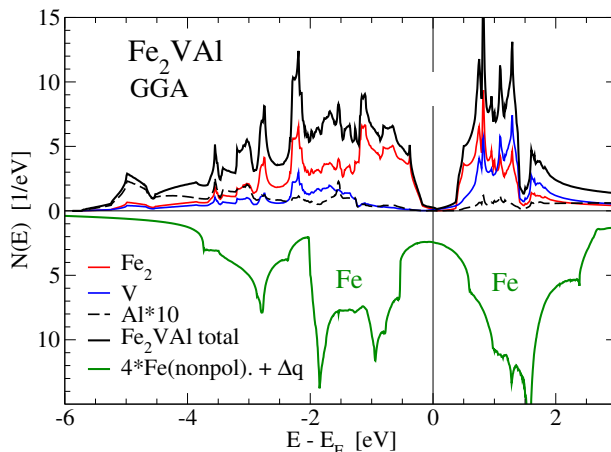


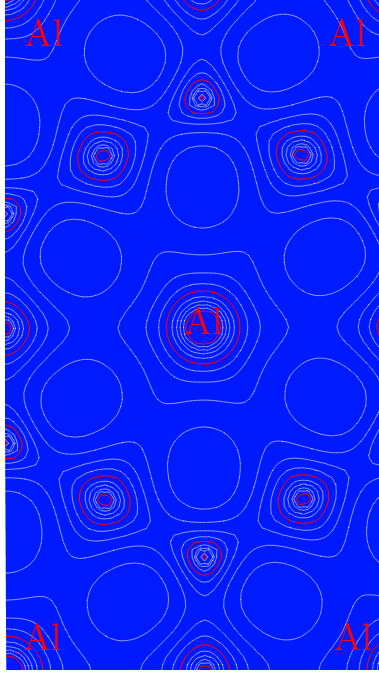
FIG. 1: Density of states  $N(E)$  for the standard GGA calculations of  $\text{Fe}_2\text{VAl}$  (upper panel) and non-spin polarized Fe (lower panel). Fermi energy (zero of energy scale) corresponds to 24 electrons for  $\text{Fe}_2\text{VAl}$ . For pure Fe in (lower panel)  $E_F$  is defined by  $4 * \int^{E_F} N(E)(E)dE = 24 - \Delta q$ . The value of  $\Delta q = 1.5$  corresponds to the total electronic charge transfer from V and Al to Fe,  $2 * \Delta q_{at}(Fe)$ , see text.

As a simple model for the DOS of the compound, in the lower panel of Fig.1, we replace all 4 atoms of  $\text{Fe}_2\text{VAl}$  by artificial Fe atoms with only 5.625 valence electrons per Fe atom. This number is obtained by subtracting 1.5 electrons (total charge transfer to Fe according to Table 1) from the 24 valence electrons of the compound,  $24 - 1.5 = 4 \times 5.625$ . By that we simulate the embedding of Fe ions in an effective medium which provides 1.5 electrons. Accordingly, for the DOS in the lower panel the Fermi energy corresponds to 22.5 valence electrons. The occurrence of the pseudogap in  $\text{Fe}_2\text{VAl}$  is already indicated for the pure Fe case because  $E_F$  falls into a very deep minimum when taking into account the charge transfer to Fe. This minimum is a well known feature of the bcc structure, separating  $t_{2g}$  and  $e_g$  states. All the shown results are done within the standard GGA approach.

### III. LOWEST CONDUCTION BAND STATE AT X

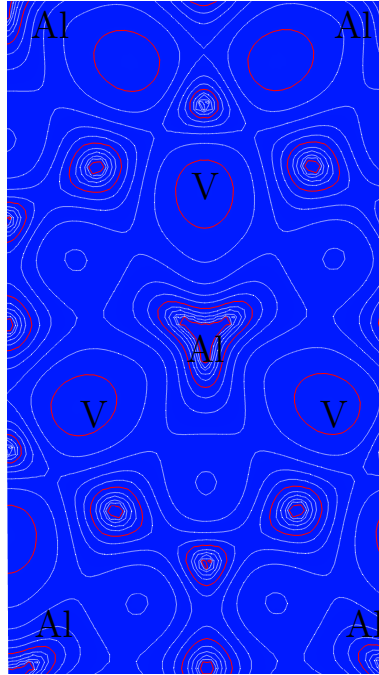
In this section the lowest conduction band state at X with its tails dangling from V to Al is visualized in terms of charge density contour plots in [111] planes. Generated by package VESTA [2].

FIG. 2: [111] plane with cut through Al-positions (red) - corresponding to  $z=0$  Å.



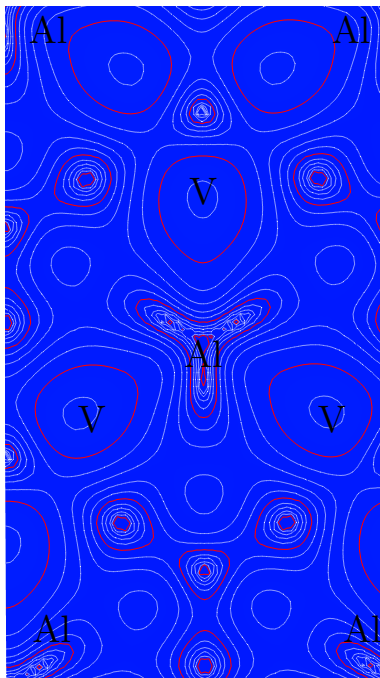
The charge density contour plot in the [111] plane through Al-positions ( $z=0$ ) (Fig. 2) shows hollow spheres around each Al position. These positions are surrounded by a triangle of V-positions which are  $0.821$  Å above the  $z=0$  plane. The tails of the electronic states centered at V merge together to form the spherically shaped charge density around Al.

FIG. 3: [111] plane  $0.068 \text{ \AA}$  above  $z=0$  plane.



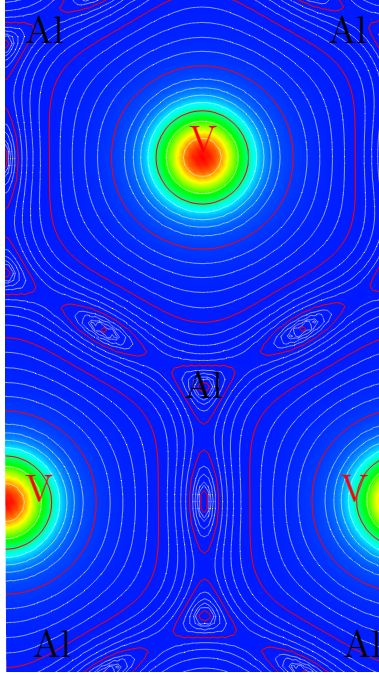
In Fig.3 moving  $z_1 = 0.068 \text{ \AA}$  above the  $z=0$  plane we cut through the dangling tails (broad tips pointing from V towards Al) which merge to a propeller like feature with distance  $z_1$  above Al. Plane orientation is [111].

FIG. 4: [111] plane  $0.137 \text{ \AA}$  above  $z=0$  plane.



In Fig.4 moving  $z_1 = 0.137 \text{ \AA}$  above the  $z=0$  plane we cut through the dangling tails (broad tips pointing from V towards Al) which merge to an even more pronounced propeller like feature with distance  $z_1$  above Al. Plane orientation is [111].

FIG. 5: [111] plane with cut through V-positions (color red) corresponding to  $z=0.821 \text{ \AA}$ .



In Fig.5 for  $z = 1.64 \text{ \AA}$  above the  $z=0$  plane we cut through centers of the V atoms with their highly localized charge density close to the nuclear positions. One realizes the rather spherical distribution of the tails around V (marked red) with small distortions towards Al, which lies below at  $z=0$ .

- 
- [1] I. Knapp, B. Budinska, D. Milosavljevic, P. Heinrich, S. Khmelevskyi, R. Moser, R. Podloucky, P. Prenninger, and E. Bauer, Phys. Rev. B **96**, 045204 (2017).  
 [2] K. Momma and F. Izumi, J. Appl. Crystallogr. **44**, 1272 (2011).